

## The effect of ferrous sulfate pretreatment on the optimal temperature for production of sugars during autothermal pyrolysis

Chad A. Peterson<sup>1</sup>, Sean S. Rollag<sup>2</sup>, Jake K. Lindstrom<sup>3</sup>, Robert C. Brown<sup>1,2,3</sup>

<sup>1</sup>*Department of Mechanical Engineering, Iowa State University, Ames, IA 50011, United States*

<sup>2</sup>*Department of Chemical and Biological Engineering, Iowa State University, Ames, IA, USA*

<sup>3</sup>*Bioeconomy Institute, Iowa State University, Ames, IA 50011, United States*

### Abstract

Fast pyrolysis is a promising technology for producing cellulosic sugars from lignocellulosic biomass. Success in this endeavor requires measures that prevent naturally occurring alkali and alkaline earth metals (AAEM) from breaking pyranose and furanose rings in lignocellulosic biomass. This is especially critical for high ash feedstocks like corn stover and other kinds of herbaceous biomass. Pretreating corn stover with ferrous sulfate converts AAEM into thermally stable salts, which passivates the catalytic activity of these metals and dramatically improves sugar yields. AAEM passivation in combination with autothermal (partial oxidative) operation improves the prospects for intensifying the production of sugars via fast pyrolysis. We hypothesized that pretreated biomass pyrolyzed in the presence of oxygen can substantially influence the temperature dependence of pyrolysis kinetics. We found that autothermal (air-blown) pyrolysis of ferrous sulfate pretreated corn stover achieved maximum sugar yield of 15.6 wt.% (biomass basis) at 450°C, whereas the maximum phenolic oil yield of 9.2 wt.% (biomass basis) was reached at 500°C. Considering these tradeoffs in yields of these highly desirable pyrolysis products, the ideal operating temperature is between 450-500°C. These results suggest that two-stage pyrolysis might allow maximum recovery of both sugars and phenolic oil.

### Keywords

Corn stover; fast pyrolysis; temperature; autothermal

## 1. Introduction

Fast pyrolysis is a promising approach for producing fuels and chemicals from lignocellulosic biomass.<sup>1–3</sup> The effect of temperature on conventional fast pyrolysis of lignocellulosic biomass is well known<sup>4</sup>, with maximum yield of bio-oil occurring around 500 °C. However, very little is known about the effect of temperature on the yield of pyrolytic sugars produced under oxidative conditions, a topic of increasing interest.<sup>3,5,6</sup>

Conventional pyrolysis of lignocellulose yields very little sugar. The inherent alkali and alkaline earth metal (AAEM) content of biomass catalyzes fragmentation of pyranose and furanose rings into light oxygenated compounds, significantly reducing sugar yield.<sup>7</sup> Extensive washing or acid impregnation to remove or passivate these metals enhance sugar production.<sup>7–9</sup> Acid pretreatment of high ash feedstocks increases sugar yields as much as ten-fold. However, AAEM content also appears to catalyze depolymerization of lignin in the biomass.<sup>10</sup> Removal or passivation of AAEM has the unintended consequence of reducing the rate of lignin devolatilization compared to its rate of melting. Unfortunately, in the absence of a depolymerization catalyst, lignin melts and dehydrates into char agglomerates, leading to reactor operability problems.<sup>11,12</sup> Char agglomeration significantly reduces reactor throughput and may even force reactor shutdown. Rollag et al.<sup>10</sup> developed an alternative pretreatment using ferrous sulfate (FeSO<sub>4</sub>) in which sulfate anions passivate AAEM while ferrous cations catalyze lignin depolymerization.<sup>13–15</sup> Pretreatment of biomass with ferrous sulfate produced pyrolytic sugar yields comparable to acid pretreatment while eliminating char agglomeration. In tests with corn stover, ferrous sulfate pretreatment dramatically shifted products from the aqueous phase (e.g. furans and other small oxygenated compounds from polysaccharides) to more valuable

anhydrosugars.<sup>10,16</sup> This substantial increase in sugar yield and reactor operability offers the prospect of large-scale production of cellulosic sugar from lignocellulosic biomass.

Conventional fast pyrolysis excludes oxygen under the assumption that bio-oil readily oxidizes at pyrolysis temperatures.<sup>17</sup> This notion seemed to be confirmed by early attempts to operate a pyrolyzer autothermally through addition of oxygen, resulting in large losses of bio-oil (>10 wt.% biomass basis).<sup>17,18</sup> Studies in our laboratory challenge this idea.<sup>16,19,20</sup> At low equivalence ratios (<10%), partial oxidation of pyrolysis products release just enough energy to provide the enthalpy for pyrolysis, making the process energy neutral. Polin et al.<sup>16,19</sup> performed similar autothermal experiments with untreated feedstocks (red oak and corn stover) measuring bio-oil losses from oxidation. Building upon this work, Rollag et al.<sup>10</sup> pyrolyzed biomass pretreated with ferrous sulfate to increase sugar yields in both inert gas and low oxygen equivalence ratio environments. These studies found autothermal pyrolysis of low-ash feedstocks pyrolyzed differently than higher ash feedstocks.<sup>10,16,19</sup> Although Polin et al.<sup>19</sup> showed that autothermal pyrolysis of woody biomass reduced the yield of heavy ends of bio-oil only by 8 wt%, they noted that among the constituents of the heavy ends, water soluble sugars were reduced about 20% and phenolic monomers reduced about 40% as a result of oxidation. Some loss in bio-oil yield is not surprising as studies of reveal that model compounds found in bio-oil can oxidize at pyrolysis temperatures.<sup>21,22</sup>

Peterson et al.<sup>23</sup> determined that high-ash feedstocks (e.g., corn stover and switchgrass) have biochar oxidation rates nearly three times that of low-ash feedstocks (red oak and pine), which was ascribed to AAEM in the ash serving as oxidation catalysts. Ferrous sulfate pretreatment to passivate AAEM and prevent it from catalyzing pyranose ring fragmentation is expected to also passivate the catalytic oxidation of biochar. However, the ferrous iron introduced to the biochar

offers an alternative oxidation catalyst, as documented by Lotz et al.<sup>24</sup> Ferrous iron likely acts in a redox cycle to oxidize biochar.<sup>25</sup>

The yield of pyrolysis products is well known to be influenced by temperature<sup>26-28</sup>, although its effect on product yields from pretreated biomass has been underexplored. A notable study by Oudenhoven et al.<sup>29</sup> found that increasing pyrolysis temperature from 360°C to 480°C increased sugar yield of acid washed pinewood from 23 wt.% to 29 wt.% (biomass basis). However, for temperatures above 530°C sugar yield decreased to less than 20 wt.%.

In addition to preventing pyranose ring fragmentation during polysaccharide deconstruction and preventing char agglomeration, we anticipate that ferrous sulfate pretreatment, by releasing ferrous cations to the char, will catalyze char oxidation, thus minimizing bio-oil losses by preferentially consuming biochar. Iron is well known to be a strong oxidation catalyst.<sup>24</sup> Previous work has shown that char oxidation is catalyzed by its ash content.<sup>23</sup> Thus, it was hypothesized that the use of ferrous sulfate as a biomass pretreatment would produce iron-rich biochar that would more readily oxidize than the organic vapors released during pyrolysis. Furthermore, by passivating AAEM in the char, gas-solid reactions between anhydrosugar vapors and the AAME will be reduced, thus boosting sugar yields.<sup>22</sup>

We hypothesize that the optimum temperature for maximum bio-oil yields from the pyrolysis of biomass pretreated with ferrous sulfate will be lower than the 500°C usually employed in fast pyrolysis of untreated biomass. At lower temperatures, secondary cracking/oxidation reactions decrease, increasing sugar yield.<sup>30</sup> Counteracting this positive effect, the yield of lignin-derived phenolic oil is likely to decrease as lignin depolymerization favors elevated temperatures.<sup>31</sup> The present study attempts to find the optimum temperature for

pyrolysis of pretreated biomass to achieve maximum oil yield. While prior works have investigated autothermal pyrolysis and pretreatment of biomass, this work merges these initiatives to maximize bio-oil yield. Likewise, this work proposes a simple, but novel, kinetic scheme of autothermal fast pyrolysis reaction kinetics to validate experimental measurements. Consequently, this work advances the understanding of ferrous sulfate pretreatment operating under autothermal conditions.

Iron-sulfate pretreated corn stover was pyrolyzed at four pyrolysis temperatures under autothermal operation. To analyze the products, numerous analytical techniques (e.g., mass spectrometry and high-performance liquid chromatography) were used to gain a better understanding of temperature effects. With the goal of maximizing sugar and phenolic oil yield, this work will aid in future scale-up of fast pyrolysis biorefineries.

## 2. Methods

### 2.1. Ferrous sulfate pretreatment

All experiments used *Zea mays* (corn stover) biomass collected using multi-pass harvesting.<sup>16</sup> The bales were initially ground using a hammer mill with a 3.2 mm screen followed by additional processing with a knife mill through a 1.6 mm screen. The ferrous sulfate treatment solution was made by dissolving the desired amount of sulfate into 1 kg of water. This solution was continuously sprayed onto the biomass with a syringe pump at a rate of 75 ml min<sup>-1</sup> to achieve a 1:1 water-to-biomass mass ratio. The mixture was mixed with a Erweka paddle mixer. Total ferrous sulfate loading was 7.5 wt. % (biomass basis), which was determined to fully passivate the AAEM content.<sup>10</sup> After pretreatment, the samples were dried at 105°C until

moisture content was below 10 wt. %. Compositional properties of the untreated corn stover can be found in Table 1.

**Table 1.** Corn stover compositional properties. All values reported as received.

<b>Proximate Analysis</b>	<b>wt. %</b>
Moisture	7.0
Volatiles	73.6
Fixed Carbon	11.1
Ash Content	8.3

<b>Ultimate Analysis</b>	<b>wt. %</b>
Carbon	40.7
Hydrogen	5.1
Sulfur	0.0
Nitrogen	0.5

## 2.2. Continuous pyrolysis reactor and fractional recovery of condensable vapors

A 3.8 cm diameter, 40 cm high bubbling fluidized bed reactor was used for the pyrolysis experiments.<sup>10</sup> The reactor was initially loaded with 600 grams of 600-1200  $\mu\text{m}$  diameter silica sand. Two cyclones immediately downstream of the reactor recovered biochar elutriated from the reactor. After the cyclones, product vapors and gases entered a staged condenser train. Stage fraction 1 (SF1) was a shell and tube heat exchanger with vapors exiting at 130°C, varying  $\pm 10^\circ\text{C}$  depending upon biomass throughput. Stage fraction 2 (SF2) was a hot electrostatic precipitator (ESP) operated at 120°C and 15 kV. The condensate collected by SF1 and SF2 were combined and referred to as the heavy ends of bio-oil. It was composed mostly of anhydrosugars and phenolic compounds.<sup>31</sup> The vapors then entered a second shell and tube heat exchanger at 0°C (SF3), followed by an ESP operated at -15°C and 15 kV (SF4). A desiccant trap downstream of SF4 removed any remaining condensable vapors. The condensate from the last two stage fractions were combined and referred to as the light ends of bio-oil. It consisted of an aqueous

solution of light organic compounds. Quantification of the non-condensable gases (NCG) was performed using a micro-GC (Varian CP-4900) with gas flow rate determined using a drum-type gas meter. Importantly, biochar yield was reported on a “ferrous sulfate-free” basis by subtracting the mass of ferrous sulfate added to the biomass prior to pyrolysis, which was incorporated into the structure of the biochar.

Nitrogen gas (from a nitrogen generator) and air flow controllers allowed equivalence ratio in the pyrolyzer to be controlled for a fixed gas flow of 20 standard liters per minute (SLPM). After initial reactor heating, biomass feed rate was started at  $0.5 \text{ kg hr}^{-1}$  for 20 minutes. Biomass feed rate was then ramped up to  $1 \text{ kg hr}^{-1}$  for 50 minutes of steady state operation. In this study, four separate reactor temperatures were investigated, with setpoints of 400, 450, 500, and 550  $^{\circ}\text{C}$ .

During autothermal operation, the energy required for pyrolysis is provided by exothermal oxidation reactions in the reactor. To determine the quantity of air required to achieve autothermal operation, air was progressively introduced into the reactor until heater output was reduced to the level required to offset parasitic heat loss.<sup>19</sup> The equivalence ratio, defined as the air flow rate over the stoichiometric amount required for complete combustion, was found to be 0.10. While the equivalence ratio was kept constant across the four temperatures used, it is possible that small differences could have existed with the required oxygen needed to sustain autothermal operation. This ratio corresponded to a gas flow rate of 5.6 SLPM of air at a biomass feed rate of  $1 \text{ kg hr}^{-1}$ . The balance of gas flow was 14.4 SLPM of nitrogen.

## 2.3. Product analysis

### 2.3.1. Liquid-liquid extractions

Phenolic compounds were recovered from stage fractions SF1 and SF2 (heavy ends) through liquid-liquid extraction. Five grams of SF1 or SF2 were mixed with equal mass of water in 50 mL centrifuge tubes. These were heated to 65°C for 20 minutes and subsequently vortexed for four minutes followed by centrifugation (Fischer Scientific accuSpin 1) at 3000 RPM for 20 minutes to achieve phase separation. The aqueous phase, containing water-soluble carbohydrates, was decanted from the water-insoluble phase and stored for subsequent high-performance liquid chromatography (HPLC) and gel filtration chromatography (GFC) analyses. The water-insoluble phase, consisting of mostly phenolic compounds, was washed with an equal mass of water, to remove any remaining water-soluble components. The water-soluble phase was decanted and stored for subsequent HPLC and GFC analyses. The use of two consecutive water washes assured complete removal of carbohydrate from the heavy ends.<sup>32</sup> The remaining insoluble phase, referred to as phenolic oil, was dried in a vacuum oven at 40°C at a pressure of 0.2 bar for 15 hours to drive off any residual moisture before subsequent chemical analysis. Any additional mass loss from vacuum drying was subsequently included in the second extract mass. Samples were analyzed in duplicate.

### 2.3.2. Ultimate Analysis

Ultimate analysis was used to determine the carbon, hydrogen, sulfur, nitrogen, and oxygen of the bio-oil stage fractions and bio-char. For each sample, 5 mg was weighed into a tin capsule and placed into an elemental analyzer (Elementar vario MICRO cube). The instrument measured mass fractions of carbon, hydrogen, sulfur, and nitrogen in a sample, with oxygen content determined by difference for the bio-oil components. All samples were prepared in duplicate or greater.<sup>33</sup> The large ash fraction of the biochar skewed oxygen content from ultimate analysis and was not reported.<sup>34</sup>

### 2.3.3. Proximate analysis

The moisture, volatile, and total inorganic (ash) contents of the biochar were determined using proximate analysis procedures in a thermogravimetric analyzer (TGA). The moisture content was determined as the mass loss of the biochar after heating to 105°C and the volatile content defined as mass loss in an inert environment upon heating to 900°C subtracting out moisture content. Fixed carbon was determined as the mass loss after the introduction of air at 900°C. Ash content was the residual material after non-oxidative and oxidative decomposition.

The ferrous sulfate treatment added additional mass to the biochar in the form of ferrous complexes and sulfate salts. Therefore, two corrections were applied to the biochar analysis to obtain results on a biomass basis. The amount of ferrous sulfate added to the biomass was 7.5 wt.%. The resulting amounts of sulfate salts and ferrous iron in the biochar were 4.74 wt.% and 2.76 wt.% on a biomass basis. These salts and cations were assumed to be completely retained in the biochar. To account for the sulfate portion, the stoichiometric amount of sulfate salts (4.74 wt.%) was subtracted from the measured volatile mass. Given that these sulfates decompose to sulfur oxide at temperatures exceeding 600°C<sup>35</sup>, their complete mass loss was assumed to occur during the proximate analysis heating from 35°C to 900°C. Likewise, the mass of ferrous iron (2.76 wt.%) was subtracted from the ash content as iron is non-volatile at 900°C.

### 2.3.4. Sugar quantification

Sugar yields were determined for SF1 and SF2 bio-oil fractions by acid hydrolysis. For this analysis, 60 mg of bio-oil was weighed into a vial followed by the addition of 6 ml of 400 mM sulfuric acid. The samples were hydrolyzed at 125°C for 44 minutes followed by rapid cooling to prevent any additional degradation reactions.<sup>36</sup> The samples were filtered using a 0.45 µm

microfiber filter into a 2 mL vial. Quantification of glucose, xylose, and sorbitol was determined with high-performance liquid chromatography (Dionex Ultimate 3000 series HPLC).<sup>37</sup> Sugar analysis was performed on four replicates of bio-oil stage fractions to overcome potential heterogeneity in the viscous samples.

Given the heterogeneity of the heavy ends, a second method for sugar quantification was performed using the aqueous sugar solution from the heavy ends of bio-oil. Using a procedure similar to sugar quantification with the heavy ends of bio-oil, 60 mg of the aqueous sugar solution from the liquid-liquid extractions (i.e., the raffinate) was weighed into a vial, then 6 mL of 400 mM sulfuric acid was added. The samples were again hydrolyzed at 125°C for 44 minutes, followed by rapid cooling. Quantification of the sugars was performed using the same HPLC method as described above. Quantifying the sugars in the liquid-liquid extract represented a quality control check on the sugars in the heavy ends.

### 2.3.5. Karl Fisher titration

The moisture content of the bio-oil was determined by Karl Fischer titration (Mettler Toledo V30S Compact Volumetric KF Titrator). For analysis of the heavy ends, approximately 70 mg of SF1 or SF2 bio-oil was dissolved in 1 mL of dry methanol (Hydranal<sup>TM</sup>). For light ends, 20 mg of each stage fraction were analyzed directly. All samples were analyzed in duplicate. Data was reported on a weight percentage basis.

## 2.4. Thermogravimetric analysis to derive ferrous sulfate treated biochar oxidation rates

Using a Mettler Toledo TGA/DSC1 (Columbus, OH, USA) thermo-gravimetric analyzer (TGA), biochar oxidation kinetics were derived for ferrous sulfate treated corn stover. The

biochar from these studies was produced in the work of Rollag et al.<sup>10</sup> The corn stover was pretreated with 7.5 wt.% of ferrous sulfate and pyrolyzed under autothermal conditions at 500°C. Biochar recovered from the cyclone separators was sieved to a particle size of 150-250µm and subjected to isothermal oxidation experiments. For these kinetic experiments, 1 mg samples in nitrogen atmospheres were temperature ramped to the desired temperature set-point, at which time the gas flow controller was switched from nitrogen to air. Oxidation of the carbonaceous biochar to CO<sub>2</sub> resulted in mass loss curve with time used to calculate biochar oxidation rates. Duplicate experiments were conducted at temperature set-points of 280, 300, 320, and 360°C to derive Arrhenius parameters. Additional studies were conducted at elevated temperatures from 366 to 566°C at 33°C intervals. Because small deviations between the set-point and actual sample temperature were observed, the internal sample temperature was used to calculate Arrhenius parameters. Details of the methodology used for the isothermal oxidation experiments can be found elsewhere.<sup>23</sup>

## 2.5. Oxidation model for select pyrolysis products in a fluidized bed reactor

Reaction rates were calculated for gaseous and solid pyrolysis components at the reactor conditions used in the physical experiments. For the gaseous components, levoglucosan and acetic acid oxidation rates were calculated from the work of Peterson et al.<sup>21</sup> with the rate coefficient calculated from an Arrhenius equation:

$$k_o = A \times \exp(-E_a/RT) \quad [1]$$

where A is the pre-exponential factor (s<sup>-1</sup>), E<sub>a</sub> is the activation energy in kJ-mol<sup>-1</sup>, T is the temperature (K), and R is the universal gas constant. For the gaseous species, it was assumed that the species were perfectly mixed, thus react at a rate equal to the intrinsic oxidation rate calculated with the Arrhenius equation.

For the oxidation of the solid biochar, the kinetic rate has to account for the mass transfer of oxygen to the surface of the biochar particle. The intrinsic/kinetic rate of the ferrous sulfate pretreated biomass biochar was calculated under a kinetically limited regime (Section 2.4). The external oxygen mass transfer rate calculation is found in the supplemental information. Briefly, the external oxygen mass transfer rate was calculated assuming a spherical 1000  $\mu\text{m}$  (particle sieve size used in this work) particle with a binary mixture of air and nitrogen. The flow rate was assumed to be 20 SLPM, and gas velocity calculated based on thermal expansion at the four reactor temperatures used in these experiments (400-550°C) from heating in the reactor calculated. Therefore, both the mass transfer rate ( $k_D$ ) and the intrinsic chemical kinetic rate ( $k_o$ ) are needed to calculate the overall biochar oxidation rate of  $k_T$ :

$$k_T = \frac{1}{\frac{1}{k_D} + \frac{1}{k_o}} \quad [2]$$

For biochar oxidation, the partial pressure of oxygen was assumed constant, and the mass transfer rate was calculated including the bulk rate and gaseous diffusion rate (assumed binary mixture of CO<sub>2</sub> and air). Additional calculations on the mass transfer rate can be found in the supplemental information.

### 3. Results

#### 3.1. Autothermal pyrolysis kinetic model

##### 3.1.1. Biochar oxidation kinetics from TGA experiments

Mass loss data from oxidation of biochars in the TGA under isothermal conditions was converted into an Arrhenius plot shown in Figure 1. As expected, oxidation rates increased for biochar produced from ferrous sulfate pretreated biomass compared to untreated biomass.

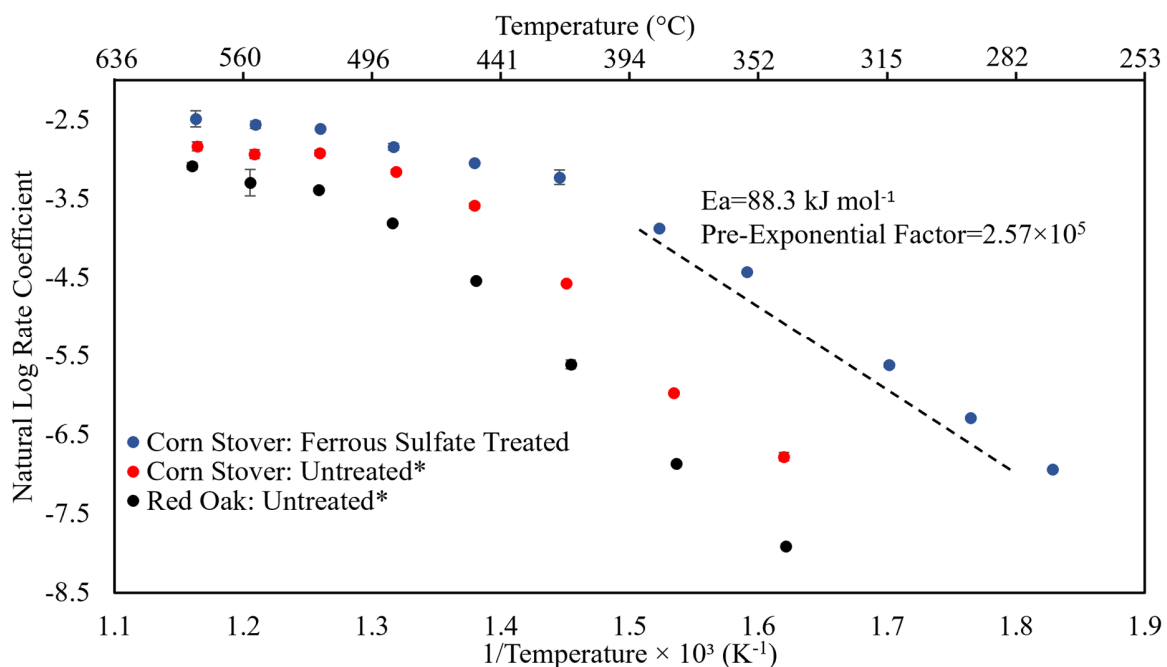


Figure 1. Oxidation kinetics for biochar produced from ferrous sulfate pretreated corn stover indicates it was substantially more reactive than biochar produced from untreated feedstocks. Error bars are the sample standard deviation from duplicate trials at each condition. Arrhenius parameters were calculated from the five lowest temperature data points for the iron sulfate biochar, as above 400°C the biochar is mass transfer limited. Untreated corn stover and red oak data reproduced from Peterson et al.<sup>23</sup>

For temperatures less than 400°C (chemical kinetic limited regime), the presence of ferrous iron increased the rate coefficient for biochar oxidation by at least an order of magnitude. Above 400°C, ferrous sulfate treated corn stover was limited by external mass transfer in the TGA rather than the intrinsic chemical kinetic rate of oxidation. This is evident from the plateaus in the data shown in Figure 1.<sup>23</sup> In contrast, the lower reactivity of the untreated feedstocks required temperatures in excess of 475°C before mass transfer limitations were evident in the data. Accordingly, Arrhenius parameters were calculated using data measured below 400°C for biochar produced from ferrous sulfate pretreated biomass to assure rate data reflected chemical kinetics. As expected, with the iron acting as an oxidation catalyst, the activation energy was

reduced from 113 kJ mol<sup>-1</sup> to 88 kJ mol<sup>-1</sup>, with the regular corn stover and ferrous sulfate treated corn stover, respectively. This catalytic effect is explored in the following sections.

### 3.1.2. Modeled oxidation rates of select pyrolysis products

Oxidation rates of select pyrolysis products were calculated from the work of Peterson et al.<sup>21</sup> and the measured oxidation rate of corn stover biochar treated with ferrous sulfate. It is hypothesized the external oxygen mass transfer rate will become the rate limiting step of biochar oxidation as pyrolysis temperature is increased above 500°C, thus preferentially oxidizing bio-oil versus biochar. To test this hypothesis, the external oxygen mass transfer rate was calculated based on bed conditions (see Supplemental Information Section 1.2 for additional model derivation), and the overall (intrinsic and mass transfer) biochar oxidation rate is compared to the calculated oxidation rates of select bio-oil products.

The implication of having the biochar oxidation rate limited by the mass transfer rate at these fluidized bed conditions can be used to determine an optimal autothermal pyrolysis reactor temperature. Peterson et al.<sup>21</sup> measured the oxidation rates for levoglucosan and acetic acid, which are plotted in Figure 2 along with the overall oxidation rate of biochar (Equation S1) produced from ferrous sulfate pretreated corn stover. For reactor temperatures above 500°C, the biochar approaches a constant value as a result of external mass transfer limitations for gas-solid reaction. Notably, the levoglucosan oxidation was only 6.2 times that of the char oxidation rate at 400 °C, however this rate more than doubles to 14.3 at 600°C. Consequently, these organic vapors would be preferentially oxidized compared to biochar at temperature above 500 °C, reducing the yield of condensable vapors (bio-oil).

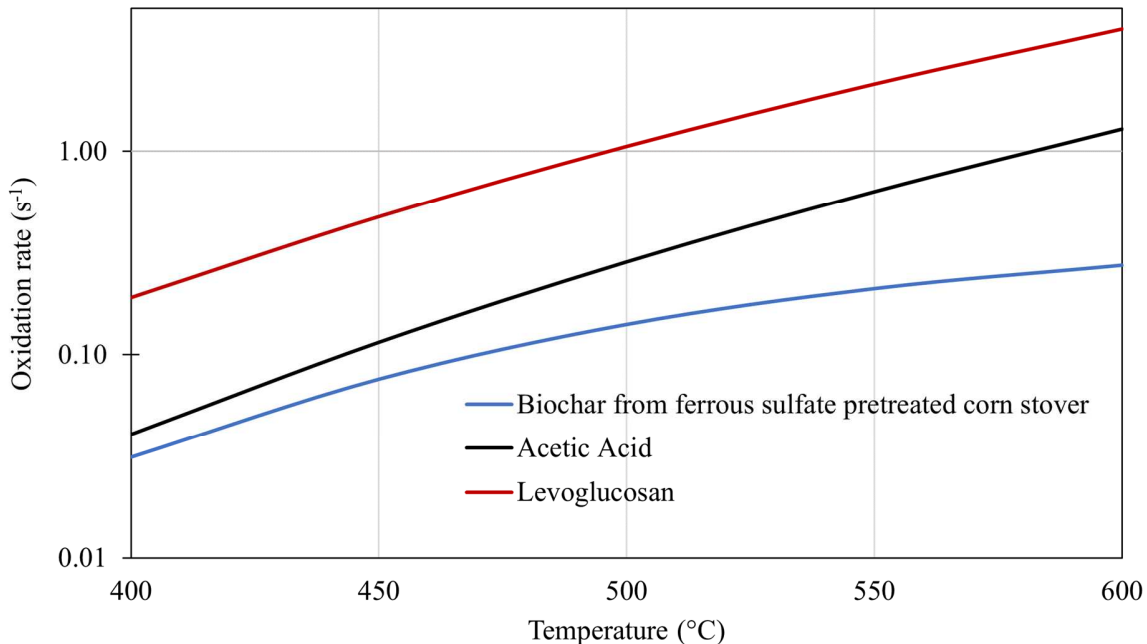


Figure 2. The oxidation rates of bio-oil products (acetic acid and levoglucosan) versus the oxidation rate of biochar produced from ferrous sulfate pretreated corn stover in a fluidized bed reactor. At temperatures above 500 °C, the oxidation rate of biochar becomes limited by external mass transfer.

These results suggest that autothermal pyrolysis of pretreated biomass be conducted at temperatures somewhat lower than 500°C to preserve bio-oil against oxidation. The influence of temperature on yield of pyrolysis products is discussed in the following sections.

### 3.2. The effect of ferrous sulfate pretreatment on products of corn stover pyrolysis as a function of temperature

Ferrous sulfate pretreated corn stover was pyrolyzed at four temperatures (400, 450, 500, and 550°C) using a fluidized bed reactor under autothermal conditions. At lower temperatures (450 and 400°C), it was hypothesized that valuable anhydrosugars would be preserved with biochar preferentially oxidized. In contrast, at elevated temperatures, it was thought sugars

would be preferentially oxidized as the biochar would be mass transfer limited (Section 3.1) favoring sugar oxidation at these fluidized bed conditions.

As shown in Figure 3, the yield of biochar from ferrous sulfate pretreated corn stover decreased from 28.8 wt. % to only 14.0 wt. % as temperature increased from 400°C to 550°C. This changes reflect the increasing depolymerization of biomass as temperature is increased.<sup>31</sup> Given the recalcitrant structure of biomass, lignin biopolymers require elevated temperatures to fully depolymerize. This is evident from previous observations that lignin-derived products increase with pyrolysis temperature.<sup>29</sup>

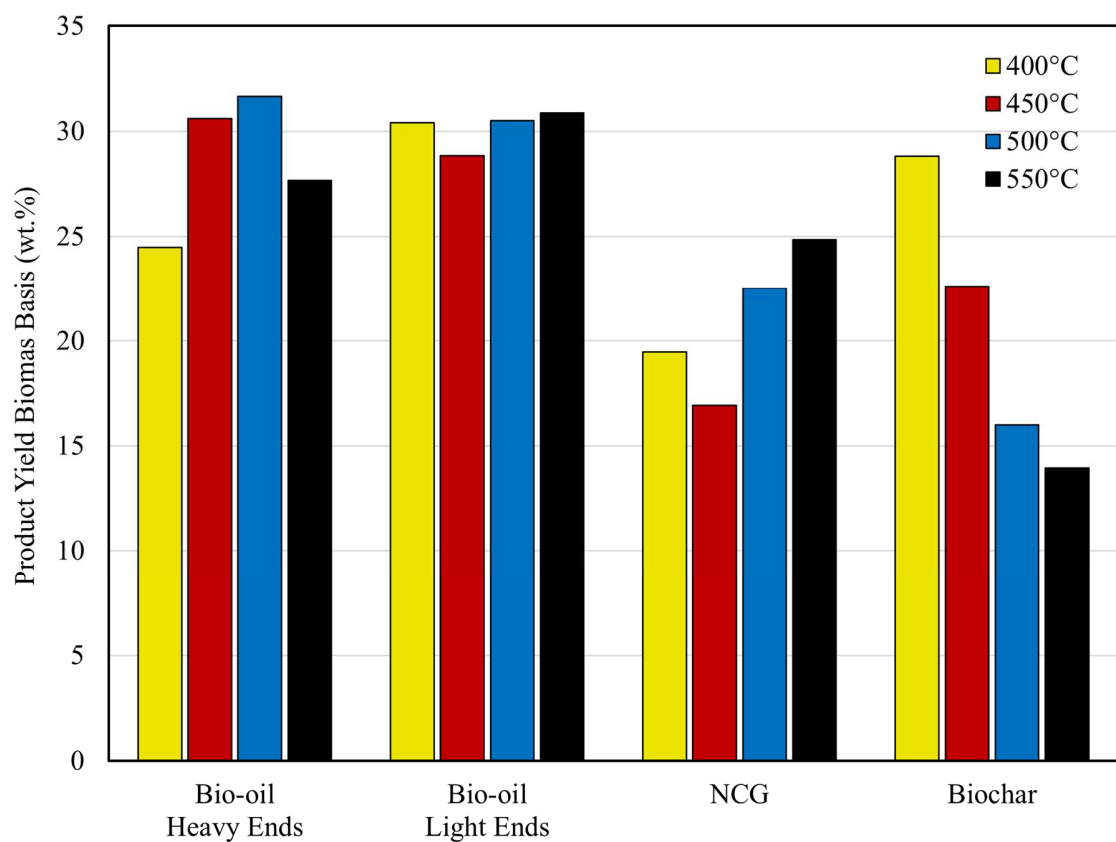


Figure 3. Yield of products as a function of temperature from autothermal pyrolysis of ferrous sulfate pretreated corn stover. Biochar and NCG yield had an inverse relationship while total bio-oil yield reached a maximum at 500°C.

Yield of total bio-oil (combined heavy ends and light ends) ranged from 54.9 to 62.2 wt. %, with the maximum yield occurring at 500°C. This result is comparable to bio-oil yields reported in the literature for conventional (non-oxidative) pyrolysis, which peak between 450-500°C.<sup>4,26,31</sup> For conventional pyrolysis, this temperature range is thought to be a balance between devolatilization of biomass and secondary cracking of bio-oil vapors. The yield of light ends (SF3 and SF4) was relatively constant with temperature (28.8-30.9 wt. %) while the yield of heavy ends (SF1 and SF2) was more dependent on temperature, ranging from 24.5-31.7 wt. % with peak yield at 500°C. Given that the heavy ends contain phenolic compounds and anhydrosugars, the variation in yield indicates that these compounds are more likely to crack than the lower molecular compounds found in the light ends.

Ultimate analysis, shown in Table 2, demonstrates that the elemental composition of heavy ends was essentially uninfluenced by temperature for ferrous sulfate pretreated corn stover. The carbon content slightly increased with temperature from 49.6 to 52.5 wt. %, with a corresponding decrease in oxygen. However, this increase in carbon content, as evaluated by Student's t-test ( $\alpha=0.05$ ), was not statistically significant. Trace amounts of sulfur were detected in the heavy ends, suggesting that a small amount of biochar (containing ferrous sulfate) may have been carried over from the cyclones to the condensers. Despite variation in bio-oil yield (24.5-31.7 wt. %), elemental composition was not statistically different. Notably, though carbon content of the light ends increased slightly with temperature, from 18% to 21.4%, this variation was not statistically significant ( $\alpha=0.05$ ).

The carbon content of biochar decreased with temperature from 46.8 to 30.9 wt. % on a biochar basis. At elevated temperatures the biopolymers undergo additional devolatilization leaving behind a greater percentage of ash in the biochar (see Section 3.3.2 for additional

**Table 2.** Elemental composition of bio-oil fractions and biochar as a function of temperature from autothermal pyrolysis of ferrous sulfate pretreated corn stover. All weight percentages are presented on as received basis. Bracket value is the sample standard deviation.

Pyrolysis Component	Temperature (°C)	Yield (g/100g biomass)	Ultimate Analysis (wt. %)					KF Moisture (%)
			Carbon	Hydrogen	Sulfur	Nitrogen	Oxygen (difference)	
Heavy Ends	400	24.5	49.6 [0.6]	5.6 [0.1]	0.2 [0.1]	0.4 [0.1]	44.2 [0.8]	5.6 [0.3]
	450	30.6	49.6 [0.9]	5.5 [0.3]	0.0 [0.1]	0.6 [0.1]	44.2 [1.1]	4.2 [0.3]
	500	31.7	51.2 [0.4]	6.0 [0.2]	0.0 [0.1]	0.7 [0.1]	42.1 [0.4]	4.3 [0.3]
	550	27.7	52.6 [0.4]	5.7 [0.2]	0.3 [0.1]	0.7 [0.1]	40.8 [0.6]	4.2 [0.1]
Light Ends	400	30.4	18.0 [0.8]	5.6 [1.6]	0.1 [0.2]	0.4 [0.2]	75.9 [2.1]	62.1 [1.5]
	450	28.8	14.6 [3.5]	5.1 [2.7]	0.1 [0.1]	0.3 [0.2]	79.9 [6.0]	64.1 [0.5]
	500	30.5	21.0 [1.0]	6.3 [1.6]	0.0 [0.1]	0.3 [0.1]	72.4 [2.5]	57.0 [0.6]
	550	30.9	21.4 [1.0]	7.3 [0.4]	0.0 [0.1]	0.4 [0.1]	71.0 [1.6]	57.6 [0.4]
Biochar	400	28.8	46.8 [0.1]	2.5 [0.1]	7.9 [0.3]	1.0 [0.1]	-	-
	450	22.6	40.5 [0.5]	2.2 [0.3]	4.2 [1.2]	1.3 [0.2]	-	-
	500	16.0	35.0 [0.2]	2.0 [0.2]	3.7 [0.1]	1.0 [0.1]	-	-
	550	14.0	33.9 [0.6]	1.4 [0.1]	9.5 [0.3]	0.9 [0.1]	-	-

discussion). As previously mentioned, biochar data is presented as received, with oxygen content not accounted for, consistent with previous work of high ash biochars.<sup>33</sup>

Of note, most of the water (>90 wt.%) was collected with the light ends. Given the operation of the condenser system, this result was expected. Additional discussion about light ends composition is found in the supplemental information.

### 3.3. Effect of ferrous sulfate pretreatment of corn stover on yield, composition, and properties of biochar and bio-oil heavy ends as a function of pyrolysis temperature

#### 3.3.1. Yield of water insoluble fraction of heavy ends

Figure 4 shows the fractions of phenolic oil and water-soluble compounds in the heavy ends as a function of temperature. The water-soluble fraction, consisting mostly of carbohydrate-derived compounds (including sugars) dominated the composition of the heavy ends, reflecting the effectiveness of the ferrous sulfate treatment in preserving the carbohydrate fraction as sugars.<sup>10</sup> Whereas the yield of water-soluble compounds peaked at 450°C, the phenolic oil reached maximum yield at 500°C. The recalcitrant nature of lignin likely requires this higher temperatures to be fully deconstructed.<sup>38</sup> Above 500°C, NCG increased at the expense of phenolic oil, suggesting that lignin oligomers were being thermally cracked to light gases or oxidized. As previously determined, any temperature increase above 500°C would only promote oxidation of condensable vapors compared to biochar. Similarly, Zhou et al.<sup>39</sup> found the yield of pyrolytic lignin (that is, the water-insoluble fraction) from untreated pine reached a maximum at 530°C, then subsequently declined at higher temperatures.

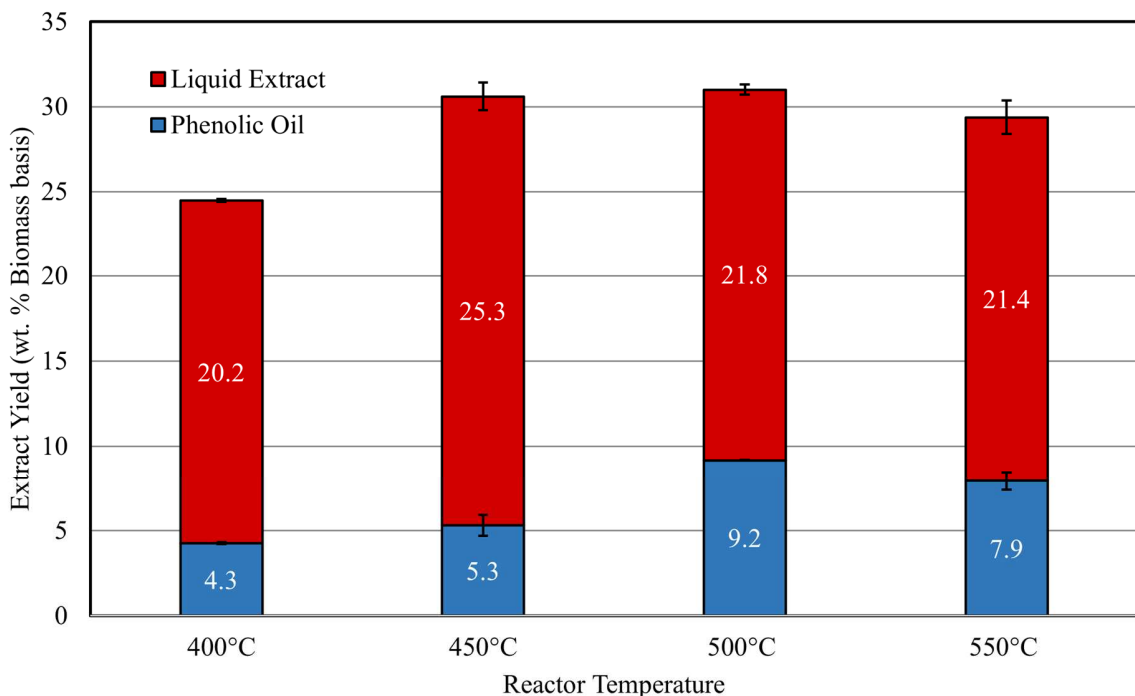


**Figure 4.** Water-soluble compound yield as a function of temperature from autothermal pyrolysis of ferrous sulfate pretreated corn stover. Yield of phenolic oil (water insoluble products) reached a maximum at 500°C. Error bars represent sample standard deviation.

### 3.3.2. Sugar yield

The maximum yield of hydrolyzable sugar occurred at 450°C (15.6 wt. %), and subsequently decreased at higher temperatures as shown in Figure 5. Gas-phase degradation and oxidation of the sugar products likely explains the decline in sugar above 450°C. Similarly, Oudenhoven et al.<sup>29</sup> observed an optimal temperature of 450°C for sugar production in their experiments with acid-leached pinewood.

Considering the strong temperature dependence of anhydrosugar degradation and oxidation, one might expect sugar yield to favor much lower pyrolysis temperatures than observed in these experiments. However, residence times of biomass particles in a fluidized bed pyrolyzer might not be long enough to fully depolymerize polysaccharides to volatile compounds at lower temperatures.<sup>38,40</sup>

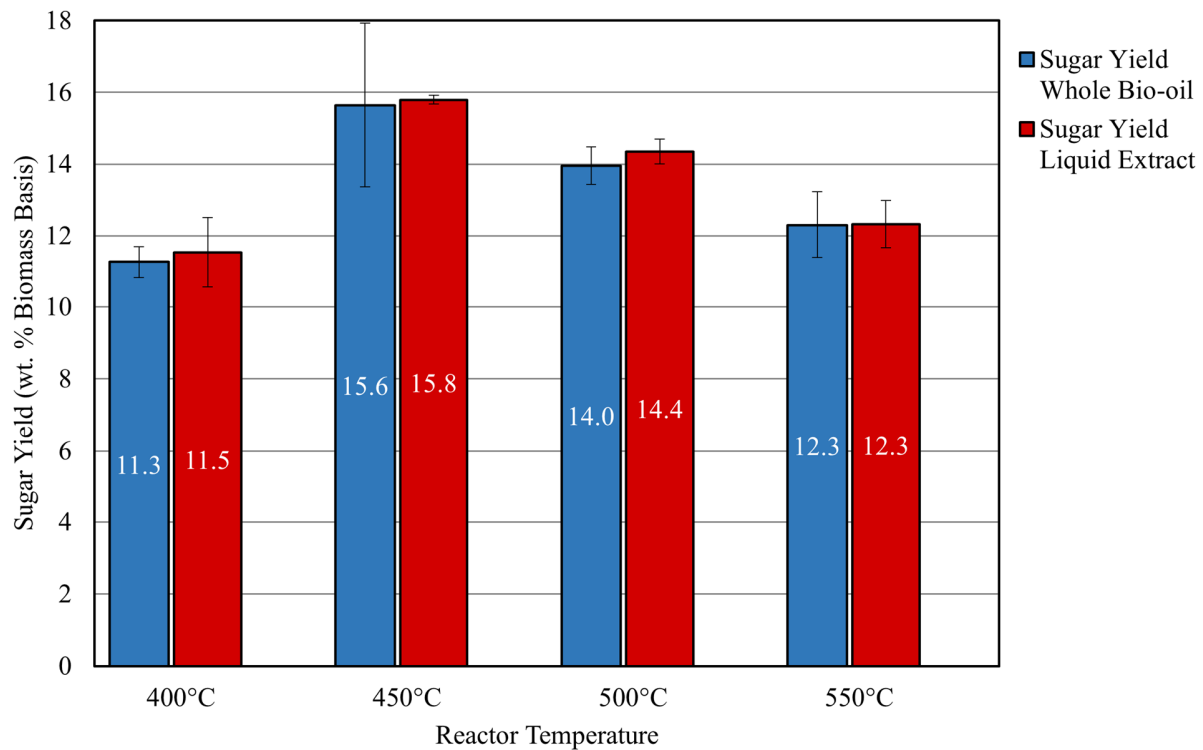


**Figure 5.** Sugar yield as a function of temperature from autothermal pyrolysis of ferrous sulfate pretreated corn stover as determined through HPLC analysis. Whole bio-oil represents direct quantification of sugar yield in heavy ends. Water-soluble yield was based on sugar concentration and mass of the liquid extract. The agreement in yield between the two indicates sugars are readily extracted during the water wash. Error bars represent sample standard deviation.

Proximate analysis found significant volatile content in biochar produced at lower reactor temperatures (Figure 6). Volatile matter increased from 1.3 wt. % to just 9.1 wt. % (biomass basis) as temperature decreased from 550°C to 400°C. Similarly, fixed carbon increased from 4.6 wt. % to 12.4 wt. % as temperature decreased from 550 to 400 °C. These results demonstrate that the biomass is almost completely devolatilized in the fluidized reactor for pyrolysis at the upper range of pyrolysis temperature, leaving behind biochar that is mostly carbonaceous solid and ash.

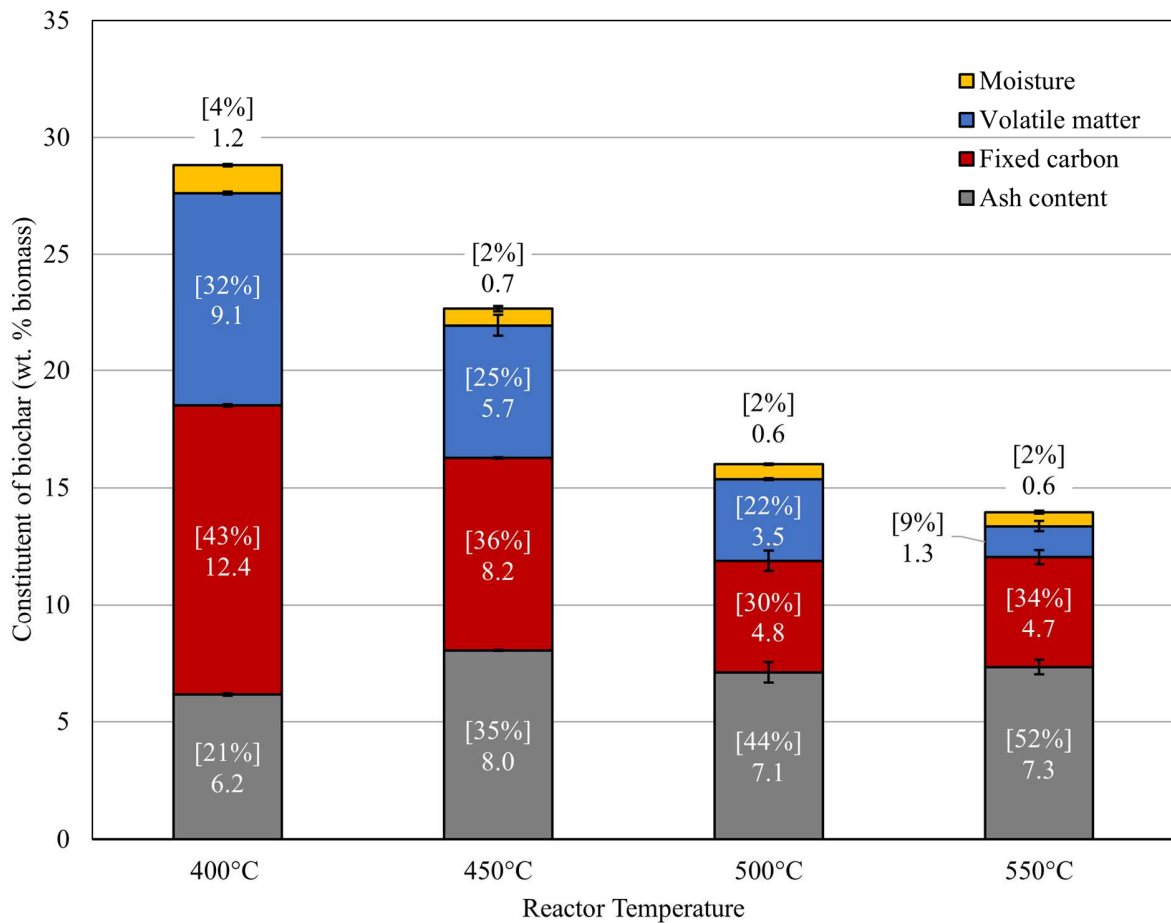


**Figure 6.** Comparison of the proximate analysis of the biochar. The component mass is reported on a biomass basis and the bracket value indicates on a biochar basis (summation of 100%). The mass of the ferrous sulfate treatment was accounted for. Error bars are sample standard deviation.

Unfortunately, temperatures that promote the production and preservation of phenolic oil are deleterious to sugar yield. Temperatures below 400°C may not be high enough to fully depolymerize the biomass while temperatures above this promote decomposition and oxidation of high molecular weight products including both anhydrosugars and phenolic compounds. As a result, there appears to be an optimum temperature of between 450-500°C for production of sugars during autothermal pyrolysis of ferrous sulfate pretreated biomass.

#### **4. Conclusion and discussion**

This work demonstrates that autothermal pyrolysis of pretreated biomass offers previously underexplored opportunities to operate at lower temperatures than conventional pyrolysis of untreated biomass. Comparison of oxidation kinetics for biochar produced from ferrous sulfate pretreated corn stover and oxidation kinetics for condensable products suggests an optimum reactor temperature of 450°C to maximize sugar production. However, the maximum yield of phenolic oil occurred at 500°C, indicating a tradeoff with temperature between production of sugars and phenolic oil.

#### **5. Acknowledgements**

This work was supported by the Department of Energy under Award Number EE0008326 and DE-AC36-08GO28308. It was prepared as an account of work sponsored by an agency of the United States Government. Neither the United States Government nor any agency thereof, nor any of their employees, makes any warranty, express or implied, or assumes any legal liability or responsibility for the accuracy, completeness, or usefulness of any information, apparatus, product, or process disclosed, or represents that its use would not infringe privately owned rights. Reference herein to any specific commercial product, process, or service by trade name, trademark, manufacturer, or otherwise does not necessarily constitute or imply its endorsement, recommendation, or favoring by the United States Government or any agency thereof. The views and opinions of authors expressed herein do not necessarily state or reflect those of the United States Government or any agency thereof.

#### **References**

(1) Brown, R. C. *Thermochemical Processing of Biomass: Conversion into Fuels, Chemicals and Power*; Brown, R. C., Ed.; John Wiley & Sons, Ltd: Chichester, UK, 2011. <https://doi.org/10.1002/9781119990840>.

(2) Pinheiro Pires, A. P.; Martinez-Valencia, L.; Tanzil, A. H.; Garcia-Perez, M.; García-Ojeda, J. C.; Bertok, B.; Heckl, I.; Argoti, A.; Friedler, F. Synthesis and Techno-Economic Analysis of Pyrolysis-Oil-Based Biorefineries Using P-Graph. *Energy & Fuels* **2021**, *35* (16), 13159–13169. <https://doi.org/10.1021/acs.energyfuels.1c01299>.

(3) Brown, R. Heterodoxy in Fast Pyrolysis of Biomass. *Energy & Fuels* **35** (2), 987–1010. <https://doi.org/10.1021/acs.energyfuels.0c03512>.

(4) Bridgwater, A. V.; Meier, D.; Radlein, D. An Overview of Fast Pyrolysis of Biomass. *Org. Geochem.* **1999**, *30* (12), 1479–1493. [https://doi.org/10.1016/S0146-6380\(99\)00120-5](https://doi.org/10.1016/S0146-6380(99)00120-5).

(5) Rover, M. R.; Aui, A.; Wright, M. M.; Smith, R. G.; Brown, R. C. Production and Purification of Crystallized Levoglucosan from Pyrolysis of Lignocellulosic Biomass. *Green Chem.* **2019**, *21* (21), 5980–5989. <https://doi.org/10.1039/C9GC02461A>.

(6) Oyedeqi, O.; Pecha, B.; Finney, C.; Peterson, C.; Smith, R.; Mills, Z.; Gao, X.; Shahnam, M.; Rogers, W.; Ciesielski, P.; Brown, R.; II, J. Cfd–Dem Modeling of Autothermal Pyrolysis of Corn Stover with a Coupled Particle- and Reactor-Scale Framework. *Chem. Eng. J.* **2022**, *446*, 136920. <https://doi.org/10.1016/j.cej.2022.136920>.

(7) Kuzhiyil, N.; Dalluge, D.; Bai, X.; Kim, K. H.; Brown, R. C. Pyrolytic Sugars from Cellulosic Biomass. *ChemSusChem* **2012**, *5* (11), 2228–2236. <https://doi.org/10.1002/cssc.201200341>.

(8) Pecha, B.; Arauzo, P.; Garcia-Perez, M. Impact of Combined Acid Washing and Acid Impregnation on the Pyrolysis of Douglas Fir Wood. *J. Anal. Appl. Pyrolysis* **2015**, *114*, 127–137. <https://doi.org/10.1016/J.JAAP.2015.05.014>.

(9) Zhou, S.; Xue, Y.; Cai, J.; Cui, C.; Ni, Z.; Zhou, Z. An Understanding for Improved Biomass Pyrolysis: Toward a Systematic Comparison of Different Acid Pretreatments. *Chem. Eng. J.* **2021**, *411*, 128513. <https://doi.org/https://doi.org/10.1016/j.cej.2021.128513>.

(10) Rollag, S. A.; Lindstrom, J. K.; Brown, R. C. Pretreatments for the Continuous Production of Pyrolytic Sugar from Lignocellulosic Biomass. *Chem. Eng. J.* **2020**, *385* (December 2019), 123889. <https://doi.org/10.1016/j.cej.2019.123889>.

(11) Dalluge, D. L.; Daugaard, T.; Johnston, P.; Kuzhiyil, N.; Wright, M. M.; Brown, R. C. Continuous Production of Sugars from Pyrolysis of Acid-Infused Lignocellulosic Biomass. *Green Chem.* **2014**, *16* (9), 4144–4155. <https://doi.org/10.1039/c4gc00602j>.

(12) Kim, K. H.; Brown, R. C.; Bai, X. Partial Oxidative Pyrolysis of Acid Infused Red Oak Using a Fluidized Bed Reactor to Produce Sugar Rich Bio-Oil. *Fuel* **2014**, *130*, 135–141. <https://doi.org/10.1016/j.fuel.2014.04.044>.

(13) Tiarks, J. A.; Dedic, C. E.; Meyer, T. R.; Brown, R. C.; Michael, J. B. Visualization of Physicochemical Phenomena during Biomass Pyrolysis in an Optically Accessible Reactor. *J. Anal. Appl. Pyrolysis* **2019**, 104667. <https://doi.org/10.1016/J.JAAP.2019.104667>.

(14) Zhou, S.; Brown, R. C.; Bai, X. The Use of Calcium Hydroxide Pretreatment to Overcome Agglomeration of Technical Lignin during Fast Pyrolysis. *Green Chem.* **2015**, *17* (10), 4748–4759. <https://doi.org/10.1039/c5gc01611h>.

(15) Rollag, S. A.; Jeong, K.; Peterson, C. A.; Kim, K. H.; Brown, R. C. An Experimental and Modeling Study on the Catalytic Effects of Select Metals on the Fast Pyrolysis of Hardwood and Softwood Lignin. *Green Chem.* **2022**, *24* (16), 6189–6199. <https://doi.org/10.1039/d1gc04837f>.

(16) Polin, J. P.; Carr, H. D.; Whitmer, L. E.; Smith, R. G.; Brown, R. C. Conventional and Autothermal Pyrolysis of Corn Stover: Overcoming the Processing Challenges of High-Ash Agricultural Residues. *J. Anal. Appl. Pyrolysis* **2019**, *143* (July), 104679. <https://doi.org/10.1016/j.jaap.2019.104679>.

(17) Li, D.; Berruti, F.; Briens, C. Autothermal Fast Pyrolysis of Birch Bark with Partial Oxidation in a Fluidized Bed Reactor. *Fuel* **2014**, *121*, 27–38. <https://doi.org/10.1016/j.fuel.2013.12.042>.

(18) Zhao, S.; Luo, Y.; Su, Y.; Zhang, Y.; Long, Y. Experimental Investigation of the Oxidative Pyrolysis Mechanism of Pinewood on a Fixed-Bed Reactor. *Energy and Fuels* **2014**, *28* (8), 5049–5056. <https://doi.org/10.1021/ef500612q>.

(19) Polin, J. P.; Peterson, C. A.; Whitmer, L. E.; Smith, R. G.; Brown, R. C. Process Intensification of Biomass Fast Pyrolysis through Autothermal Operation of a Fluidized Bed Reactor. *Appl. Energy* **2019**, *249*, 276–285. <https://doi.org/10.1016/J.APENERGY.2019.04.154>.

(20) Kim, K. H.; Bai, X.; Rover, M.; Brown, R. C. The Effect of Low-Concentration Oxygen in Sweep Gas during Pyrolysis of Red Oak Using a Fluidized Bed Reactor. *Fuel* **2014**, *124*, 49–56. <https://doi.org/10.1016/j.fuel.2014.01.086>.

(21) Peterson, C. A.; Brown, R. C. Global Gas-Phase Oxidation Rates of Select Products from the Fast Pyrolysis of Lignocellulose. *Energy & Fuels* **2021**, *35* (21), 17103–17113. <https://doi.org/10.1021/acs.energyfuels.1c01207>.

(22) Plouffe, C.; Peterson, C. A.; Rollag, S. A.; Brown, R. C. The Role of Biochar in the Degradation of Sugars during Fast Pyrolysis of Biomass. *J. Anal. Appl. Pyrolysis* **2022**, *161* (May 2022), 105416. <https://doi.org/10.1016/j.jaap.2021.105416>.

(23) Peterson, C. A.; Brown, R. C. Oxidation Kinetics of Biochar from Woody and Herbaceous Biomass. *Chem. Eng. J.* **2020**, *401* (June), 126043. <https://doi.org/10.1016/j.cej.2020.126043>.

(24) Lotz, K.; Berger, C. M.; Muhler, M. Catalytic Effect of Iron Phases on the Oxidation of Cellulose-Derived Synthetic Char. *Energy Procedia* **2019**, *158*, 694–699. <https://doi.org/10.1016/j.egypro.2019.01.188>.

(25) Cheng, J.; Zhou, F.; Xuan, X.; Liu, J.; Zhou, J.; Cen, K. Comparison of the Catalytic Effects of Eight Industrial Wastes Rich in Na, Fe, Ca and Al on Anthracite Coal Combustion. *Fuel* **2017**, *187*, 398–402. <https://doi.org/10.1016/j.fuel.2016.09.083>.

(26) Mourant, D.; Lievens, C.; Gunawan, R.; Wang, Y.; Hu, X.; Wu, L.; Syed-Hassan, S. S. A.; Li, C. Z. Effects of Temperature on the Yields and Properties of Bio-Oil from the Fast Pyrolysis of Mallee Bark. *Fuel* **2013**, *108*, 400–408.

<https://doi.org/10.1016/j.fuel.2012.12.018>.

(27) Garcia-Perez, M.; Wang, X. S.; Shen, J.; Rhodes, M. J.; Tian, F.; Lee, W. J.; Wu, H.; Li, C. Z. Fast Pyrolysis of Oil Mallee Woody Biomass: Effect of Temperature on the Yield and Quality of Pyrolysis Products. *Ind. Eng. Chem. Res.* **2008**, *47* (6), 1846–1854. <https://doi.org/10.1021/ie071497p>.

(28) Amutio, M.; Lopez, G.; Artetxe, M.; Elordi, G.; Olazar, M.; Bilbao, J. Influence of Temperature on Biomass Pyrolysis in a Conical Spouted Bed Reactor. *Resour. Conserv. Recycl.* **2012**, *59*, 23–31. <https://doi.org/10.1016/j.resconrec.2011.04.002>.

(29) Oudenhoven, S. R. G. R. G.; Lievens, C.; Westerhof, R. J. M. J. M.; Kersten, S. R. A. R. A. Effect of Temperature on the Fast Pyrolysis of Organic-Acid Leached Pinewood; the Potential of Low Temperature Pyrolysis. *Biomass and Bioenergy* **2016**, *89*, 78–90. <https://doi.org/10.1016/j.biombioe.2015.12.019>.

(30) Fukutome, A.; Kawamoto, H.; Saka, S. Kinetics and Molecular Mechanisms for the Gas-Phase Degradation of Levoglucosan as a Cellulose Gasification Intermediate. *J. Anal. Appl. Pyrolysis* **2017**, *124*, 666–676. <https://doi.org/10.1016/J.JAAP.2016.12.010>.

(31) Rover, M. R.; Johnston, P. A.; Whitmer, L. E.; Smith, R. G.; Brown, R. C. The Effect of Pyrolysis Temperature on Recovery of Bio-Oil as Distinctive Stage Fractions. *J. Anal. Appl. Pyrolysis* **2014**, *105*, 262–268. <https://doi.org/10.1016/j.jaap.2013.11.012>.

(32) Rover, M. R.; Johnston, P. A.; Jin, T.; Smith, R. G.; Brown, R. C.; Jarboe, L. Production of Clean Pyrolytic Sugars for Fermentation. *ChemSusChem* **2014**, *7* (6), 1662–1668. <https://doi.org/10.1002/cssc.201301259>.

(33) Brewer, C. E.; Schmidt-Rohr, K.; Satrio, J. A.; Brown, R. C. Characterization of Biochar from Fast Pyrolysis and Gasification Systems. *Environ. Prog. Sustain. Energy* **2009**, *28* (3), 386–396. <https://doi.org/10.1002/ep.10378>.

(34) Bakshi, S.; Laird, D. A.; Smith, R. G.; Brown, R. C. Capture and Release of Orthophosphate by Fe-Modified Biochars: Mechanisms and Environmental Applications. *ACS Sustain. Chem. Eng.* **2021**, *9* (2), 658–668. <https://doi.org/10.1021/acssuschemeng.0c06108>.

(35) Tagawa, H. Thermal Decomposition Temperatures of Metal Sulfates. *Thermochim. Acta* **1984**, *80* (1), 23–33. [https://doi.org/10.1016/0040-6031\(84\)87181-6](https://doi.org/10.1016/0040-6031(84)87181-6).

(36) Bennett, N. M.; Helle, S. S.; Duff, S. J. B. Extraction and Hydrolysis of Levoglucosan from Pyrolysis Oil. *Bioresour. Technol.* **2009**, *100* (23), 6059–6063. <https://doi.org/10.1016/j.biortech.2009.06.067>.

(37) Johnston, P. A.; Brown, R. C. Quantitation of Sugar Content in Pyrolysis Liquids after Acid Hydrolysis Using High-Performance Liquid Chromatography without Neutralization. *J. Agric. Food Chem.* **2014**, *62* (32), 8129–8133. <https://doi.org/10.1021/jf502250n>.

(38) Lindstrom, J. K. Analyzing and Exploiting Biomass Thermal Deconstruction, Iowa State University, 2019.

(39) Zhou, S.; Garcia-Perez, M.; Pecha, B.; Kersten, S. R. A. A.; McDonald, A. G.; Westerhof, R. J. M. M. Effect of the Fast Pyrolysis Temperature on the Primary and Secondary Products of Lignin. *Energy and Fuels* **2013**, *27* (10), 5867–5877.

<https://doi.org/10.1021/ef4001677>.

(40) Gable, P.; Brown, R. C. Effect of Biomass Heating Time on Bio-Oil Yields in a Free Fall Fast Pyrolysis Reactor. *Fuel* **2016**, *166*, 361–366.  
<https://doi.org/10.1016/J.FUEL.2015.10.073>.